DOI: 10.61782/fa.2023.1014

forum acusticum 2023

# SOUND INSULATION OF SUSPENDED CEILINGS: A FEM-BASED COMPARISON OF SUSPENSION SYSTEMS

**Jesse Lietzén**[1*] **Ville Kovalainen**[1] **Lauri Talus**[1]
**Mikko Kylliäinen**[1] **Aitor Lopetegi**[2] **Ander Aldalur**[2]
[1] AINS Group, Department of Acoustical Engineering, Finland
[2] AMC Mecanocaucho, Spain

## ABSTRACT

Measurement results for a laboratory concrete slab and differently suspended plasterboard ceilings make evident that it is beneficial to equip the ceilings with elastic suspension systems to improve both airborne and impact sound insulation of the floor. In comparison to the rigid hangers, the weighted sound reduction index $R_w$ improved 7 dB and the weighted normalized impact sound pressure level $L_{n,w}$ decreased with 15 dB when elastic hangers were used in the suspension system. The greater improvement values were achieved with the hangers including elastomer. To further study this issue and to ease the comparison of elastic and rigid hangers even in the low-frequency range, models applying the finite element method (FEM) and parametric calculation models were created. Results achieved with the validated models were used to predict improvement of sound insulation gained with the suspended ceilings. The models were used to study the phenomena affecting the performance of the different suspension systems. Results confirm the efficiency of the elastic hangers in comparison with the rigid ones. Replacing the rigid hangers with elastic hangers improved the ceiling performance with more than 10 dB, and the improvement was prominent even at very low frequencies.

**Keywords:** *suspended ceiling, elastic hangers, sound insulation, finite element method, digital acoustics laboratory.*

[*] ***Corresponding author***: *jesse.lietzen@ains.fi.*


## 1. INTRODUCTION

Suspended ceilings are an often-applied solution to improve sound insulation between overlapping spaces, and they are also used in different room-within-a-room applications. In general, the suspended ceiling systems consist of three essential parts: 1) one or several layers of building boards, 2) a frame behind the boards for the board installation, and 3) a suspension system, i.e., hangers attached to the frame to support the ceiling from the bearing floor slab. Frequently, the building boards used in the system are plasterboards or wood-based board products, and the frame consist of metal or timber profiles. The hangers used to suspend the ceiling are either *elastic* or *rigid* (i.e., very stiff in comparison with the elastic hangers). Together, these parts form an airspace between the bearing structure and the ceiling, which is usually attenuated, e.g., with a mineral wool.

To simplify the acoustical behavior of the solution, the suspended ceiling together with the bearing structure, either a concrete or a timber slab, constructs a mass-spring-mass system. Again, two different behavior types can be identified from the system, namely the acoustical coupling between the bearing structure and the ceiling boards through the (attenuated) airspace, and the mechanical coupling of the respective parts via the hangers and the frame [1]. If the airspace is sufficiently attenuated and large, the sound insulation of the structure will mostly be limited by the mechanical coupling rather than the airspace [1].

An appealing solution to improve both airborne and impact sound insulation performance of a suspended ceiling is to use an elastic suspension system. This way, the mechanical coupling through the hangers can be reduced and the sound insulation of the entire floor structure improved. According to laboratory measurements on a concrete slab [2-3], the improvement of sound insulation achieved with the ceiling

increased, when elastic hangers were used instead of rigid ones. The improvement was apparent in the frequencies above 100 Hz.

The purpose of this paper is to further study the behavior of differently suspended ceilings and to ease the comparison of hangers even in the low-frequency range below 100 Hz. This has been carried out with simulations where the abovementioned phenomena were investigated. We created simulations applying *the finite element method* (FEM) and *parametric calculation models* to predict both airborne and impact sound insulation of a laboratory concrete slab with two differently suspended ceilings. In addition to rigid hangers, the ceilings were suspended with elastomer hangers.

## 2. MATERIALS AND METHODS

### 2.1 Suspended ceilings

#### *2.1.1 Studied floor structures*

We studied the sound insulation of two floors F1 and F2 equipped with suspended plasterboard ceilings installed below a laboratory concrete slab (Fig. 1). Two plasterboards of thickness 13 mm were hanged from a 140 mm thick concrete slab with different suspension systems: rigid hangers (F1), and elastic elastomer hangers (AMC Mecanocaucho Akustik Rapid LC + Sylomer 20) (F2). The elastomer within the hanger had dimensions of 25 x 28 x 41.5 mm. In the studied cases, the air gap between the concrete slab and the plasterboard was 130 mm including a 100 mm layer of mineral wool. We also assessed a bare reference concrete slab (F0) to study the improvement of the sound insulation (both $\Delta R$ and $\Delta L$) achieved with the ceilings, and a floor F3 equipped with the ceiling without any mechanical coupling between the layers.

The configuration of the structures F1–F2 was otherwise the same in all situations but the type of the hanger changed. The hangers were attached to the concrete slab by threaded steel rods with diameters of 6 mm. The spacing of the hangers was 1200 mm along the metal frames and 600 mm in the perpendicular direction corresponding the frame spacing. The height of the metal frame was 18 mm and width 45 mm. The plasterboards ($m'$ = 9 kg/m$^2$) were attached to the metal frames with screws.

The rigid hangers were relatively stiff, but the elastomer hangers acted elastically. The natural frequency $f_0$ (of a mass-spring system) for the elastomer hanger was 11.5 Hz, when the mass per hanger was 8.5 kg. This mass corresponds the total mass from the plasterboards divided for each 32 hangers in the ceiling. Spring constant for the elastomer hanger was 44 400 N/m.

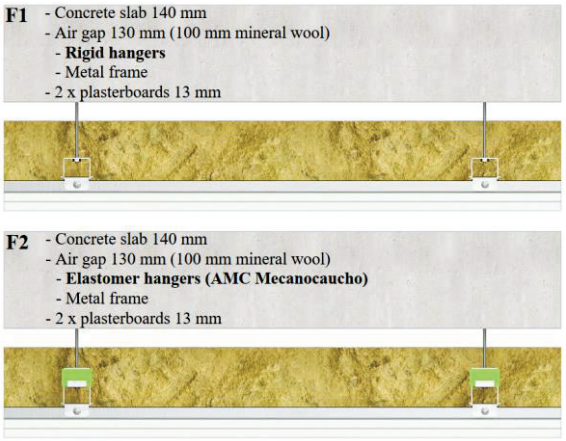


**Figure 1.** Floor structures F1 and F2. Additionally, a mechanically fully uncoupled floor F3 was studied.

#### *2.1.2 Improvement of sound insulation with the ceilings*

Previously, the airborne and impact sound insulation of structures similar to the floors F0–F2 have been measured by a building acoustics laboratory [2-3]. To distinguish the measured structures from the studied ones, the measured floors were denoted as F0 lab…F2 lab, respectively. The floor F1 lab., however, differed from the studied floors here in that the air gap between the concrete slab and the plasterboards was 100 mm, and the hanger spacing was 600 mm in both directions [2]. In this case, the measurements were carried out in the frequency range 100–5000 Hz [2]. For the structures F0 lab. and F2 lab., the measured frequency range was 50–5000 Hz [3].

Based on the laboratory measurements [2-3], improvements of the sound insulation gained with the suspended ceilings were determined for F1–F2 lab. Measurement results for the improvement of sound reduction index ($\Delta R$) have been illustrated in Fig. 2 and for the reduction in impact sound pressure level ($\Delta L$) in Fig. 3. Additionally, Figs. 2 and 3 give the improvement in single-number quantities (SNQs) $\Delta R_w$ and $\Delta L_w$ according to standards ISO 717-1 [4] and 717-2 [5]. The weighted sound reduction index $R_w$ of the bare slab F0 lab. was 56 dB and the weighted normalized impact sound pressure level $L_{n,w}$ 77 dB.

According to the Figs. 2 and 3, the results for $\Delta R$ and $\Delta L$ are highly dependent of the suspension system. The improvements in SNQs $\Delta R_w$ and $\Delta L_w$ were 7 and 15 dB higher for the ceiling of the floor F2 where the elastic suspension system was used in comparison to the rigid one

(F1). These differences cannot fully be justified with the differences of the ceiling configurations discussed above.

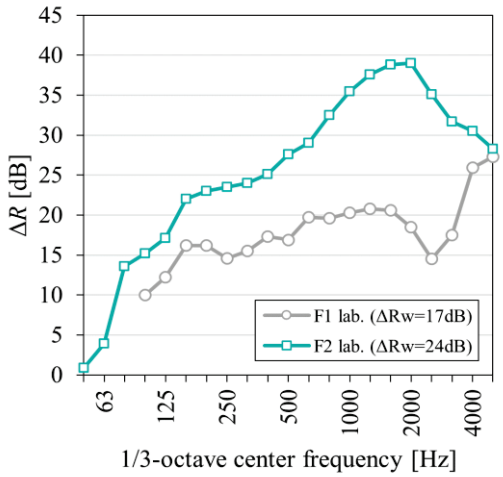


**Figure 2**. Measured improvement of sound reduction index $\Delta R$ and $\Delta R_w$ for the ceilings of the floor structures F1–F2 lab.

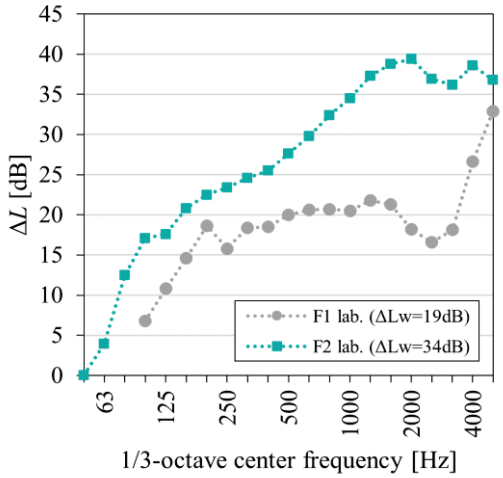


**Figure 3**. Measured reduction in impact sound pressure level $\Delta L$ and $\Delta L_w$ for the ceilings of the floor structures F1–F2 lab.

### 2.2 Simulation procedures and model descriptions

The airborne and impact sound insulation of the floor structures F0–F3 was evaluated through simulations. The simulation models were used to study the phenomena affecting the acoustical performance of the three different suspension systems. The simulations were carried out by applying FEM using COMSOL Multiphysics 6.1 in the 1/3-octave frequencies 50–200 Hz and supplemented with parametric calculation models for airborne and impact sound insulation developed by AINS Group in the 1/3-octave frequencies 250–5000 Hz.

#### *2.2.1 FEM simulations*

The FEM simulations were performed in frequency domain by applying a fully coupled multiphysics problem with a two-way interaction between the structural and acoustical domains. In the structural domains, i.e., concrete structures, plasterboards and metal parts, the governing partial differential equation of motion (without the volume force part) was:

$$\nabla \cdot \boldsymbol{S} = -\rho\omega^2\mathbf{u} \tag{1}$$

where $\boldsymbol{S}$ is the second Piola-Kirchoff stress tensor, $\rho$ is material density, $\omega = 2\pi f$ is the angular frequency, and $f$ is frequency, and $\mathbf{u}$ is the displacement [6].
The governing equation in the acoustical domains (airspaces) was the Helmholtz equation:

$$\nabla \cdot \left(-\frac{1}{\rho_0}\nabla p\right) - \frac{\omega^2 p}{\rho_0 {c_0}^2} = 0 \tag{2}$$

where $p$ is the time-harmonic sound pressure, and $\rho_0$ and $c_0$ denote the air density (1.21 kg/m$^3$) and the speed of sound in air (343 m/s), respectively [7]. Additionally, the poroacoustical domains, namely the mineral wool inside the airspace of the suspended ceilings, were modelled as an equivalent fluid by applying the modified Allard and Champoux model [7-8]. Thus, the Helmholtz equation governed also in the poroacoustical domains, but the Eqn. (2) was solved with modified complex values for the density and speed of sound in the material.
In addition to the model of the structures, the FEM models included a half-infinite receiving airspace below the structures to solve the sound power radiation directly with FEM. The fully absorptive boundary conditions for the airspace were achieved with perfectly matched layers.
First, the models were applied to solve the sound reduction index $R$. The upper surface of the concrete slab was excited with a diffuse sound field as a boundary load by generating a sum of $N$ plane waves with random phases and an even distribution over a half sphere over the surface [9] with sound power $P_{dif}$. The model was used to solve the sound power $P_{rad,air}$ radiating into the receiving airspace below structures. The sound reduction index was determined as:

$$R = 10 \log\left(\frac{P_{\text{dif}}}{P_{\text{rad,air}}}\right) \quad (3)$$

Secondly, the FEM models were used to evaluate the normalized impact sound pressure level $L_n$ of the floor structures. The floors were excited by point forces representing the impact force excitation generated by the ISO tapping machine [10]. The sound power $P_{\text{rad,imp}}$ radiated by the structure was solved, and the normalized impact sound pressure level was determined as:

$$L_n = 10 \log\left(\frac{P_{\text{rad,imp}}}{P_0}\right) + 10 \log\left(\frac{A_{\text{ref}}}{A_0}\right) \quad (4)$$

where $P_0 = 10^{-12}$ W is the reference sound power, and $A_{\text{ref}}$ and $A_0$ denote the reference sound absorption areas of 4 and 10 m$^2$, respectively. Thus, a perfectly diffuse sound field in the receiving room was assumed.

*2.2.2 Parametric calculation models*

Parametric calculation models by AINS Group were applied to evaluate both the airborne and impact sound insulation of the structures in the high-frequency range. The parametric calculation method combines different models found in literature based mostly on statistical energy analysis, lumped mechanical models and/or forced transmission approaches. The parametric model applied in this case for the airborne sound insulation is based on refs. [1,11-15]. The model takes into account, e.g., the mass and stiffness of structural layers, absorption materials inside the structure, the stiffness of studs and frames. The parametric calculation model for the impact sound insulation is based on refs. [16-20]. In addition to the abovementioned features of the parametric model for the airborne sound insulation, the impact sound insulation model considers the force interaction between the ISO tapping machine and the floor.

### 2.3 Simulations

The computational models were validated by comparing the simulation and measurement results on the bare floor structure F0 and the floor F2 with elastically suspended ceiling (presented in ref. [3]). The validated models were further applied to simulate the sound insulation of the floors F1, and F3. Elastic material properties for all the parts in the floors were not available, but the parameter values (density $\rho$, elastic modulus $E$, Poisson's ratio $\nu$, structural loss factor $\eta_s$) presented in Table 1 were applied in the simulations to model the structural parts as isotropic elastic materials. Additionally, it was presumed that the static airflow resistivity of the mineral wool was 15 000 Pa·s/m$^2$. Most of the materials in the FEM simulations were modelled as solid domains, however, the metal frames were modelled with shell elements. As an example, the computed displacements of the floor structures F0 and F2 have been illustrated in Fig. 4.

**Table 1.** Applied elastic material properties.

| Material | $\rho$ [kg/m$^3$] | $E$ [MPa] | $\nu$ [-] | $\eta_s$ [-] |
|---|---|---|---|---|
| Concrete | 2 320 | 30 000 | 0.2 | 0.006* |
| Plasterboard | 720 | 2 600 | 0.3 | 0.01 |
| Steel** | 7 850 | 210 000 | 0.3 | 0.005 |

*) Total loss factor was fit in validation to match airborne sound insulation measurement.
**) Metal frames and steel in hangers.

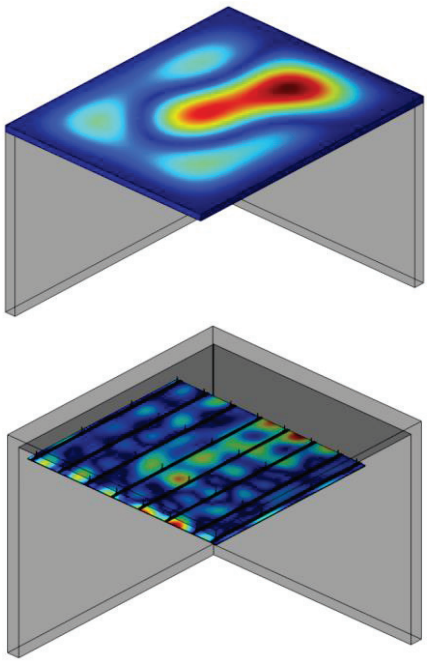

**Figure 4.** Simulated displacements of the bare floor structure F0 (above) and the floor F2 with the suspended ceiling (below) at 100 Hz, when the concrete slab was excited with diffuse sound field.

The mesh of the FE-model was built using both hexahedral and tetrahedral quadratic elements. A frequency dependent mesh was used, where the mesh size was a fifth of the wavelength of sound in air according to [7].
The wall structures connected to the concrete floor structure were modelled according to the measurement reports [2-3].

The walls were rigidly connected to the concrete floor structure. The steel studs were connected to the plasterboard by a bonded line contact along the centerline of the stud. The plasterboard layers were connected to each other by a no separation contact between the board surfaces.

To account for the ceiling hangers in the FEM models, spring-damper components were applied to connect the metal frames to the concrete slab, as previously done by Kohrmann et al. [21-22]. The validity of the simple spring-dampers was assessed by comparing the acceleration amplitudes of mass-spring systems for the fully modelled elastomer hangers and by replacing the models with the spring-damper components (Fig. 5). According to the comparison, the equivalency between the full and simple models was reasonable. The peak in Fig. 5 represents the $f_0$ of the modelled systems (rigid mass of 8.5 kg at the end of the hanger) for the elastomer hanger. In the case of the rigid hanger, the respective $f_0$ was 322,5 Hz.

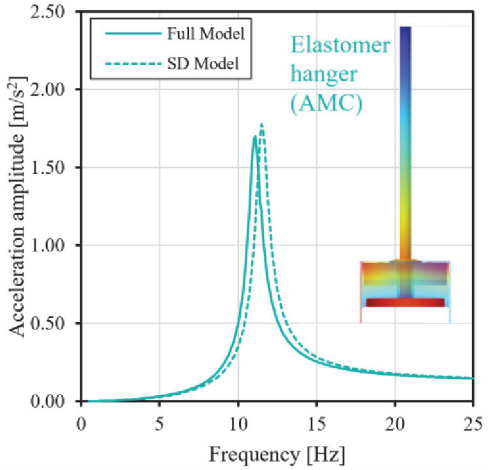


**Figure 5.** Acceleration amplitude comparison of fully modelled and spring-damper (SD) elastomer hanger (AMC) together with the simulated displacement at the resonance frequency $f_0$.

## 3. RESULTS

### 3.1 Validation results

Comparison between the simulated and measured sound reduction indices $R$ of the floor structures F0 and F2 has been shown in Fig. 6, and for the normalized impact sound pressure $L_n$ in Fig. 7. The comparisons show that the simulation models enabled accurate evaluation of the sound insulation of the bare floor. The measured and simulated $R_w$ differed 1 dB and 4 dB in case of floors F0 and F2, respectively. The respective differences for $L_{n,w}$ were 0 dB and 2 dB. Slight discrepancies between the simulation and measurement results for the $L_n$ were prominent in the low and mid-frequencies. In case of $R$, the differences were minor, but at their highest in the mid-frequencies. Due to the good correspondences, the simulation models for the $R$ and $L_n$ were regarded as valid.

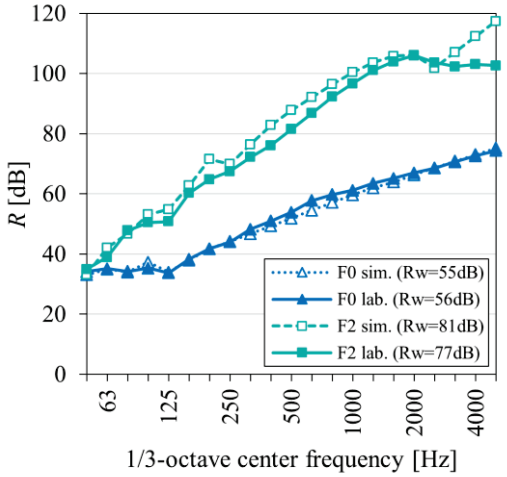


**Figure 6.** Validation results of the floor structures F0 and F2 for sound reduction index $R$ and $R_w$.

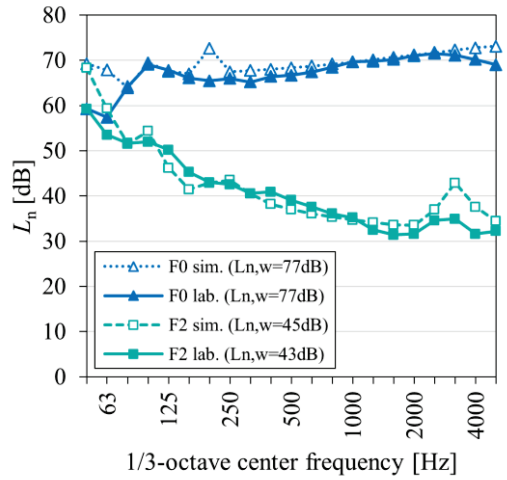


**Figure 7.** Validation results of the floor structures F0 and F2 for normalized impact sound level $L_n$ and $L_{n,w}$.

### 3.2 Improvement of sound insulation

The validated models for F0 were further applied to simulate the behavior of the suspended ceilings. The

derived improvement of sound reduction index $\Delta R$ and reduction in impact sound pressure level $\Delta L$ have been shown in Figs. 8 and 9, respectively, to illustrate the performance of the ceilings for the floors F1–F3. The weighted sound insulation improvement values presented in the figures were calculated according to the standard series ISO 717 [4, 5]. The hangers were modelled as spring-damper components as discussed in Section 2.3.

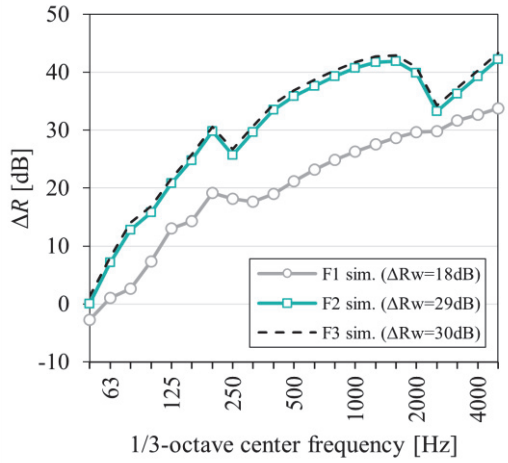


**Figure 8.** Simulated improvement of sound reduction index $\Delta R$ and $\Delta R_w$ for the ceilings of the floor structures F1–F3.

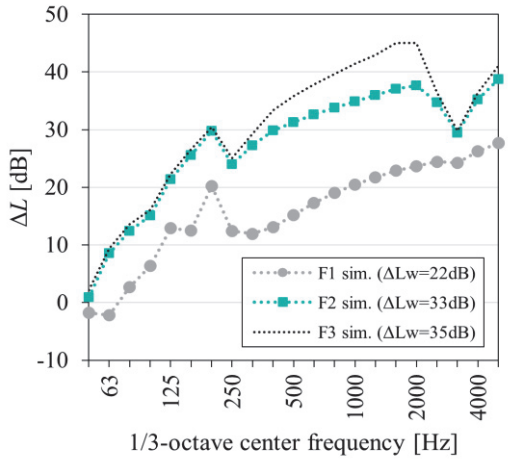


**Figure 9.** Simulated reduction in impact sound pressure level $\Delta L$ and $\Delta L_w$ for the ceilings of the floor structures F1–F3.

The results presented in the Figs. 8 and 9 show distinctive differences between the performance of rigid and elastic suspensions systems. The elastic hangers enable over 10 dB improvement to the performance of the suspended ceilings in comparison with the rigid hangers. The differences are prominent in the frequency range 50–5000 Hz. In case of elastic hangers, the differences in $\Delta R$ and $\Delta L$ were minor because of the close values for $f_0$. However, it is notable that the simulated $\Delta R$ and $\Delta L$ values were greatest for the elastomer hanger and close to the performance of the mechanically fully uncoupled ceiling (F3).

In case of the elastomer hanger, also a full 3D model of the hanger was applied in FEM simulations for sound reduction index $R$ to study the low-frequency behavior of the hanger in comparison with the spring-damper components. In the low frequencies between 50–200 Hz, the differences between the $\Delta R$ and $\Delta L$ of the elastically suspended and the fully uncoupled ceilings were approximately 1 dB (Figs. 10 and 11). It is also evident that the rigid hangers decrease the $\Delta R$ values above 50 Hz.

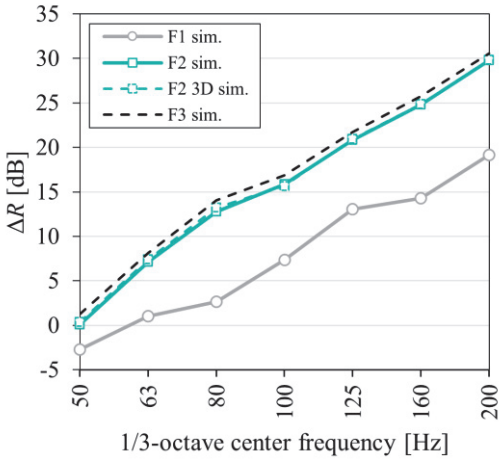


**Figure 10.** Simulated improvement of sound reduction $\Delta R$ in low frequencies for the ceilings of the floors F1–F3.

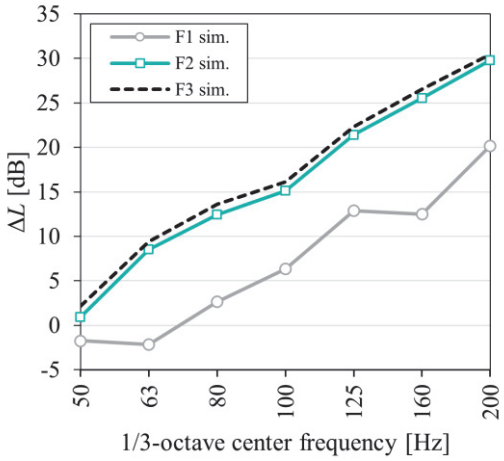


**Figure 11.** Simulated improvement of sound reduction $\Delta L$ in low frequencies for the ceilings of the floors F1–F3.

## 4. DISCUSSION

The measured sound reduction indices $R$ of the floor structure F2 were rather high and close to maximum measurable values obtainable at the facility above 400 Hz [3]. This could indicate that flanking sound transmission may alter the overall performance measured and hence lower the achieved sound insulation values in the laboratory. Moreover, measuring such high sound reduction indices demands great sound power levels in the sending room. The presented measurements for the floor structure F1 [2] are not fully comparable with the newer measurement of structure F2 since the overall cavity thickness and the hanger spacing was different. However, based on the measurement results it is evident that $\Delta R$ and $\Delta L$ were close to each other.

The simulated sound insulation improvements $\Delta R$ and $\Delta L$ (Figs. 8 and 9) were comparable with the measurement results (Figs. 2 and 3) for the floor F2 even though it should be noted that exact material parameters and dimensions were not known in all respects.

An idealized point-point connection involving spring-damper components proved to accurately describe the hanger behavior in low frequencies (Fig. 10). The inclusion of an accurate elastomer hanger geometry (in F2 3D) did not affect the improvement $\Delta R$ below 200 Hz. Thus, simplifying the hanger geometry (and probably the material parameters) into an ideal spring-damper seemed justified in the low-frequency range. Only minor differences are observed between elastic suspension systems. The stiff hanger system F1 will differ from other simulations starting at 50 Hz, but more prominently at 63 Hz.

Using the parametric models requires simplifications to the real geometries of the floor structures F1 and F2. The parametric model can not accurately describe a connection between plates (concrete slab – plasterboards) where connecting force is not symmetric and the ceiling frames are not accounted for. Hence, a moderate estimation is most likely achieved. The uncertainties caused by the simplifications can be seen from $\Delta R$ and $\Delta L$ results (Figs. 8 and 9) around the coincidence frequency of the plasterboards in the 1/3-octave bands 2500–3150 Hz. Additionally, uncertainty is assumed to involve the possible frequency-dependent material characteristics.

## 5. CONCLUSIONS

In this paper, we assessed the sound insulation behavior of two differently suspended ceilings and compared the results to the performance of the fully uncoupled ceiling. According to the results, it is beneficial to suspend the ceilings with elastic hangers. This improves the ceiling performance with more than 10 dB, and the improvement is prominent even at very low frequencies. Thus, the results confirm the efficiency of the elastic hangers in comparison with the rigid ones. By using the different modelling techniques (spring-damper components and fully modelled hangers) it was observed that at least the lowest resonance frequency of the hangers should be known when designing suspended ceilings. However, differences in geometry and elastic material properties between hanger models may become a more prominent and important factor when especially high sound insulation values are to be achieved. In case of the ceiling suspended with the studied elastomer hangers (F2), the addition of accurate geometry had no effect on the $\Delta R$ and $\Delta L$ results.

## REFERENCES

[1] B.H. Sharp: "Prediction methods for the sound transmission of building elements," *Noise Control Engineering Journal,* vol. 11, pp 53-63, 1978.

[2] M. Vidal and M. Villenave: *Rapport d'essais n° AC98-127 Concernant un plancher avec des variants de plafonds.* Marne-la-Vallée: Centre Scientifique et Technique du Bâtiment (CSTB), 1999.

[3] C. Catoire and M. Magnin: *Rapport d'essais acoustiques n°* AC19-26079642-1 *Concernant un plancher avec et sans plafond.* Marne-la-Vallée:

Centre Scientifique et Technique du Bâtiment (CSTB), 2020.

[4] EN ISO 717-1:2020: *Acoustics - Rating of sound insulation in buildings and of building elements - Part 1: Airborne sound insulation*. Brussels: European Committee for Standardization, 2020.

[5] EN ISO 717-2:2020: *Acoustics - Rating of sound insulation in buildings and of building elements - Part 2: Impact sound insulation*. Brussels: European Committee for Standardization, 2020.

[6] COMSOL: *Structural Mechanics Module User's Guide*, 2021.

[7] COMSOL: *Acoustics Module User's Guide*, 2021.

[8] J.F. Allard and Y. Champoux: "New empirical equations for sound propagation in rigid frame fibrous materials," *Journal of the Acoustical Society of America,* vol. 91, no. 6, pp. 3346–3353, 1992.

[9] B. Rafaely: "Spatial-temporal correlation of a diffuse sound field," *Journal of the Acoustical Society of America*, vol. 107, no. 6, pp. 3254-3258, 2000.

[10] V. Wittstock: "On the spectral shape of the sound generated by standard tapping machines," *Acta Acustica United with Acustica*, vol. 98, no. 2, pp. 301–308, 2012.

[11] E.C. Sewell: "Transmission of reverberant sound through a single leaf partition surrounded by an infinite rigid baffle," *Journal of Sound and Vibration,* vol. 12, pp. 21-32, 1970.

[12] J. Kristensen and J.H. Rindel: *Bygningsakutik – teori og praksis.* Glostrup: Statens Byggeforskningsinstitut, SBI-anvisning 166, 1989.

[13] EN ISO 12354-1:2017: *Building acoustics -Estimation of acoustic performance of buildings from the performance of elements – Part 1: Airborne sound insulation between rooms*. Brussels: European Committee for Standardization, 2017.

[14] V. Hongisto: *Monikerroksisen seinärakenteen ilmaääneneristävyyden ennustemalli*. Helsinki: Työterveyslaitos, Työympäristötutkimuksen raporttisarja 2, 2003.

[15] P. Virjonen and V. Hongisto: "Joustavarankaisen levyrakenneseinän äänenläpäisy," in *Proc. of the Akustiikkapäivät* (Vaasa, Finland by Akustinen Seura ry), 2009.

[16] EN ISO 12354-2:2017: *Building acoustics – Estimation of acoustic performance of buildings from the performance of elements – Part 2: Impact sound insulation between rooms*. Brussels: European Committee for Standardization, 2017.

[17] J. Brunskog and P. Hammer: "The interaction between the ISO tapping machine and lightweight floors," *Acta Acustica united with Acustica*, vol. 89, pp. 296-308, 2003.

[18] J.H. Rindel: *Sound Insulation in Buildings*. CRC Press, 2018

[19] C. Hopkins: *Sound Insulation*. Oxford: Butterworth-Heinemann, 2007

[20] L. Cremer, M. Heckl and B.A.T. Petersson: *Structure-borne sound, structural vibrations and sound radiation at audio frequencies*. Berlin: Springer-Verlag, 2005.

[21] M. Kohrmann, M. Buchschmid, G. Müller, R. Völtl and U. Schanda: "Numerical models for the prediction of vibro-acoustical characteristics of light-weighted ceilings", in *Proc. of the Inter-noise* (Innsbruck, Austria), no. 710, 2013

[22] M. Kohrmann: *Numerical Methods for the Vibro-Acoustic Assessment of Timber Floor Constructions*. Technische Universität München, Dissertation, Germany, 2017.